Model-Independent Calculation of Radiative Neutron Capture on Lithium-7

Gautam Rupak and Renato Higa

Phys. Rev. Lett. **106**, 222501 — Published 31 May 2011

DOI: 10.1103/PhysRevLett.106.222501

Model-Independent Calculation of Radiative Neutron Capture on Lithium-7

Gautam Rupak [a*] and Renato Higa [b†]
[a] *Department of Physics & Astronomy and High Performance Computing Collaboratory, Mississippi State University, Mississippi State, MS 39762, U.S.A.*
[b] *Kernfysisch Versneller Instituut, Theory Group, University of Groningen, 9747AA Groningen, The Netherlands*

The radiative neutron capture on lithium-7 is calculated model independently using a low energy halo effective field theory. The cross section is expressed in terms of scattering parameters directly related to the S-matrix element. It depends on the poorly known p-wave effective range parameter r_1. This constitutes the largest uncertainty in traditional model calculations. It is explicitly demonstrated by comparing with potential model calculations. A single parameter fit describes the low energy data extremely well and yields $r_1 \approx -1.47$ fm^{-1}.

PACS numbers: 25.40.Lw, 25.20.-x

Introduction: Low energy nuclear reactions play a crucial role in Big Bang Nucleosynthesis (BBN), stellar burning and element synthesis at supernova sites [1–3]. These low energy reactions also play an important role in testing astrophysical models and physics beyond the Standard Model of particle physics. Often the key nuclear reactions occur at energies that are not directly accessible in terrestrial laboratories. Radiative proton capture on beryllium $^7\mathrm{Be}(p,\gamma)^8\mathrm{B}$ is one of them —it is important for boron-8 production in the sun, whose weak decay results in the high energy neutrinos that are detected at terrestrial laboratories looking for physics beyond the Standard Model. The relevant solar energy, the Gamow peak, for this reaction is around 20 keV [4]. This necessitates extrapolation to solar energies of known experimental capture cross sections from above around 100 keV. Theoretical input becomes necessary for this extrapolation. Effective field theory (EFT) is an ideal formalism for this as it provides a model-independent calculation with reliable error estimates.

In an EFT, one identifies the relevant low energy degrees of freedom and constructs the most general interactions allowed by symmetry without modeling the short distance physics. The interactions are organized in a low momentum expansion. At a given order in the expansion, a finite number of interactions has to be considered and an *a priori* estimate of the theoretical error can be made. Establishing theoretical errors is crucial due to astrophysical demands [1, 2, 4]. A systematic expansion of interactions is important because many processes involve external currents, and any prescription used in phenomenological models involve some uncertainty. As an example, the cross section for $n(p,\gamma)d$ at BBN energies was calculated within EFT to an accuracy of about 1% [5]. Systematic treatment of two-body currents was necessary to achieve this level of precision, and it addressed a critical need [1] for nuclear theory input in astrophysics.

While applications of EFT to systems with $A \lesssim 4$ nucleons is well developed, for $A \gtrsim 5$ it is still in its infancy. However, some loosely bound systems, like halo nuclei open new possibilities. The small separation energy of the valence nucleons in halo nuclei provides a small expansion parameter for constructing a halo EFT [6]. In Ref [7], electromagnetic transition in the halo system ^{11}Be was considered. The ^{8}B nucleus with a proton weakly bound to the ^{7}Be core by 0.1375 MeV is a halo system. Current extrapolation of the $^7\mathrm{Be}(p,\gamma)^8\mathrm{B}$ cross section to solar energies introduce errors in the $5-20\%$ range [4, 8, 9]. A model-independent EFT calculation would be very useful to estimate the errors in the extrapolation. In addition, this would be an important step in developing EFT techniques for weakly-bound nuclei as has been accomplished in the few nucleon systems. Experiments such as those planned at the future FRIB [10] would explore exotic nuclei near the drip lines where halo systems abound. Structure and reactions with halo EFT can serve as benchmark for phenomenological models of nuclei near the drip lines.

We consider the low energy reaction $^7\mathrm{Li}(n,\gamma)^8\mathrm{Li}$, which is an isospin mirror to $^7\mathrm{Be}(p,\gamma)^8\mathrm{B}$. The n-^{7}Li system allows formulating the EFT for the nuclear interactions without the added complication of the Coulomb force. Besides, $^7\mathrm{Li}(n,\gamma)^8\mathrm{Li}$ is a key process in inhomogeneous BBN models. Its reaction rate impacts the abundance of ^{7}Li and the production of carbon-oxygen-nitrogen in the early universe, thus constraining alternative astrophysical scenarios [11]. Traditionally $^7\mathrm{Li}(n,\gamma)^8\mathrm{Li}$ has been calculated in a single-particle approximation as a ^{7}Li core plus a valence neutron interacting via a Woods-Saxon potential, e.g. Refs. [8, 12, 13]. This approximation breaks down at higher energies when the internal structure of the ^{7}Li core is probed, for example, near the threshold for $^7\mathrm{Li}(\gamma,^3\mathrm{He})\alpha$ which is about 0.5 MeV above the binding energy $B \approx 2.03$ MeV of the ^{8}Li core. We treat the ^{7}Li nucleus as point-like since we work at very low energies. In the following we show that the capture cross section below ~ 100 keV is very sensitive to the p-wave effective range r_1, a result that carries over to the mirror $^7\mathrm{Be}(p,\gamma)^8\mathrm{B}$ reaction.

Interaction: The relevant low energy nuclear degrees of freedom, here, are the point-like neutron, ^{7}Li and ^{8}Li with spin-parity $\frac{1}{2}^+$, $\frac{3}{2}^-$ and 2^+ respectively. At low energies the relevant partial waves in the incoming n-^{7}Li state are s-waves: $^3S_1$, $^5S_2$ in the spectroscopic notation $^{2S+1}L_J$. The ground state is a 2^+ state that is primarily the symmetric combination of the possible p-wave states $^3P_2$ and $^5P_2$ [14]. Conservation of parity implies that the reaction $^7\mathrm{Li}(n,\gamma)^8\mathrm{Li}$ proceeds through the electric dipole transition E1 at lowest order.

The leading order interactions for s-wave contain no derivatives. The two-component spin-$\frac{1}{2}$ neutron field $N(x)$ and four-

component spin-$\frac{3}{2}$ ^{7}Li field $C(x)$ can be combined into the $^3S_1$ and $^5S_2$ states using the Clebsch-Gordan coefficient matrices F_i, Q_{ij} as $N^T F_i C$ and $N^T Q_{ij} C$ respectively. The vector index in F_i relates to the three magnetic quantum numbers in the spin $S=1$ channel. The symmetric, traceless matrices Q_{ij} relate to the five magnetic quantum numbers in the spin $S=2$ channel. We write the s-wave leading order interaction Lagrangian as

$$\mathcal{L}^{(s)} = g^{(1)}(N^T F_i C)^\dagger (N^T F_i C) + g^{(2)}(N^T Q_{ij} C)^\dagger (N^T Q_{ij} C), \quad (1)$$

where a single momentum-independent interaction in each of the $^3S_1$ and $^5S_2$ channels was kept. The higher derivative terms are suppressed at low energy. The 2×4 Clebsch-Gordan matrices are given as

$$F_i = -\frac{i\sqrt{3}}{2}\sigma_2 S_i, \qquad Q_{ij} = -\frac{i}{\sqrt{8}}\sigma_2[\sigma_i S_j + \sigma_j S_i], \quad (2)$$

where Si's are spin-$\frac{1}{2}$ to spin-$\frac{3}{2}$ transition matrices [6] and σ_i's are the usual Pauli matrices.

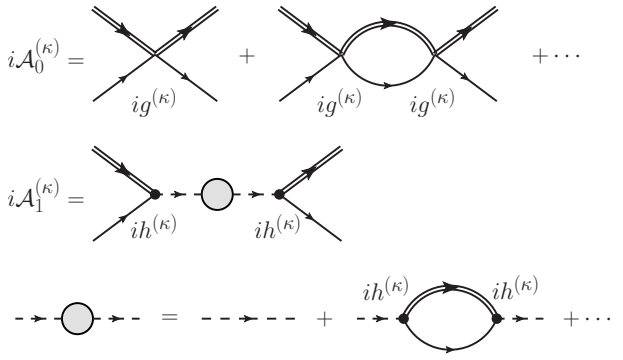

FIG. 1. $\mathcal{A}_0^{(\kappa)}$ is the $^3S_1$, $^5S_2$ scattering amplitude. $\mathcal{A}_1^{(\kappa)}$ is the $^3P_2$, $^5P_2$ scattering amplitude. Double line is the ^{7}Li propagator, single line the neutron propagator, dashed line the bare dimer propagator.

The interaction in Eq. (1) produces a s-wave amplitude shown in Fig. 1. It is a geometric series, summed to give

$$i\mathcal{A}_{EFT}^{(\kappa)}(p) = \frac{ig^{(\kappa)}}{1 - ig^{(\kappa)}L(p)},$$
$$L(p) = -i\int \frac{d^{D-1}\boldsymbol{q}}{(2\pi)^{D-1}}\frac{2\mu\,(\lambda/2)^{4-D}}{q^2 - p^2 - i0^+} = -\frac{i\mu}{2\pi}(\lambda + ip), \quad (3)$$

where $g^{(\kappa)}$ corresponds to $g^{(1)}$, $g^{(2)}$ in the respective spin channels and λ is the renormalization scale. The loop integral $L(p)$ is evaluated in the power divergence subtraction scheme [15] where divergences in both $D=4$ and lower space-time dimensions are subtracted. Matching Eq. (3) to the low-energy effective range expansion (ERE) amplitude fixes the EFT couplings as $g^{(\kappa)}(\lambda) = (2\pi)/[\mu(\lambda - 1/a_0^{(\kappa)})]$ with the scattering lengths $a_0^{(2)} = -3.63 \pm 0.05$ fm, $a_0^{(1)} = 0.87 \pm 0.07$ fm [16]. Introduction of the renormalization scale λ allows for a systematic expansion of the different terms even though the final amplitude is independent of λ [17]. In Ref. [18], initial state interactions using ERE was also considered.

The final ^{8}Li bound state is in a p-wave that we consider shallow similar to its isospin mirror ^{8}B nucleus. The EFT for shallow p-wave states was formulated in Ref. [6] where it was shown that, unlike s-wave, it requires not one but two non-perturbative EFT interactions. The renormalization of loops is easily accomplished in the dimer formalism. The interactions in the $^3P_2$ and $^5P_2$ states are constructed by combining the matrices F_i, Q_{ij} and the Galilean invariant velocity difference vector $(\boldsymbol{v}_C - \boldsymbol{v}_N)_k$ into a p-wave dimer with total $J=2$. We write the corresponding interaction Lagrangian as

$$\begin{aligned}\mathcal{L}^{(p)} =& \phi_{ij}^\dagger\left[\Delta^{(1)} + \left(i\partial_0 + \frac{\nabla^2}{2M}\right)\right]\phi_{ij} \\ &+ \sqrt{3}h^{(1)}\left[\phi_{ij}^\dagger N^T F_x\left(\frac{\overrightarrow{\nabla}}{M_C} - \frac{\overleftarrow{\nabla}}{M_N}\right)_y C + h.c.\right] R_{ijxy} \\ &+ \pi_{ij}^\dagger\left[\Delta^{(2)} + \left(i\partial_0 + \frac{\nabla^2}{2M}\right)\right]\pi_{ij} \\ &+ \frac{h^{(2)}}{\sqrt{2}}\left[\pi_{ij}^\dagger N^T Q_{xy}\left(\frac{\overrightarrow{\nabla}}{M_C} - \frac{\overleftarrow{\nabla}}{M_N}\right)_z C + h.c.\right] T_{xyzij}, \quad (4)\end{aligned}$$

where ϕ_{ij} (π_{ij}) is the dimer in the $^3P_2$ ($^5P_2$) channel, and

$$\begin{aligned}R_{ijxy} &= \frac{1}{2}[\delta_{ix}\delta_{jy} + \delta_{iy}\delta_{jx} - \frac{2}{3}\delta_{ij}\delta_{xy}], \\ T_{xyzij} &= \frac{1}{2}\left[\varepsilon_{xzi}\delta_{yj} + \varepsilon_{xzj}\delta_{yi} + \varepsilon_{yzi}\delta_{xj} + \varepsilon_{yzj}\delta_{xi}\right]. \quad (5)\end{aligned}$$

The interactions in $\mathcal{L}^{(p)}$ are equivalent to the ones with only neutron-core short range interactions without a dimer field. In terms of Feynman diagrams, the four-fermion neutron-core interaction is replaced in the dimer formulation by a dimer exchange, Fig. 1. The non-perturbative iteration of the leading operators is accomplished by "dressing" the dimer propagator with nucleon-core loops. For a given spin-channel $\kappa = 1$ ($^3P_2$) or $\kappa = 2$ ($^5P_2$) the dressed dimer propagator, which is proportional to the elastic amplitude, reads

$$\begin{aligned}iD^{(\kappa)}(p_0,\boldsymbol{p})R_{ijmn} =& \frac{iR_{ijmn}}{\Delta^{(\kappa)} - \frac{1}{2\mu}\zeta^2 + \frac{2h^{(\kappa)2}}{\mu}f(p_0,\boldsymbol{p})}, \\ f(p_0,\boldsymbol{p}) =& \frac{1}{4\pi}\left(\zeta^3 - \frac{3}{2}\zeta^2\lambda + \frac{\pi}{2}\lambda^3\right), \quad (6)\end{aligned}$$

where $\zeta = \sqrt{-2\mu p_0 + \mu p^2/M - i0^+}$, $M = M_N + M_C$. Matching the EFT amplitudes to the p-wave ERE expansion determines the coupling pair ($\Delta^{(\kappa)}$, $h^{(\kappa)}$). Again, only the first two ERE parameters are kept in the low energy expansion since EFT requires two operators at leading order.

Radiative capture: The leading order capture cross section can be calculated via minimally coupling the photon by gauging the ^{7}Li core momentum $\boldsymbol{p}_C \to \boldsymbol{p}_C + Z_C e\boldsymbol{A}$, where $Z_C = 3$ is the ^{7}Li core charge. The E1 contribution comes from the diagrams in Fig. 2. The center of mass (CM) kinematics are defined with $\boldsymbol{p}$ ($\boldsymbol{k}$) the core (photon) momentum and

$\hat{\boldsymbol{k}}\cdot\hat{\boldsymbol{p}}=\cos\theta$. Formally we take $p\sim\gamma$ as the small scale where $\gamma=\sqrt{2\mu B}\approx 57.8$ MeV is the ^{8}Li binding momentum. Then at leading order the Mandelstam variable $s\approx(M_N+M_C)^2=M^2$ and $|\boldsymbol{k}|=k_0\approx(p^2+\gamma^2)/(2\mu)$. We get for the CM differential cross section

$$\frac{d\sigma}{d\phi d\cos\theta}=\frac{1}{64\pi^2 s}\frac{|\boldsymbol{k}|}{|\boldsymbol{p}|}|\mathcal{M}|^2\approx\frac{1}{64\pi^2M^2}\frac{p^2+\gamma^2}{2\mu p}|\mathcal{M}|^2. \quad (7)$$

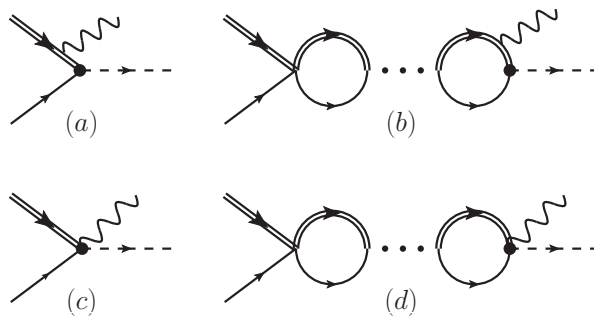

FIG. 2. Capture reactions ^{7}Li$(n,\gamma)^8$Li. Wavy lines represent photons. "$\cdots$" represents initial state s-wave interaction.

The capture from the initial state $^5S_2$ to the $^5P_2$ final state (spin channel 2) dominates due to the larger initial state scattering length $a_0^{(2)}>a_0^{(1)}$. The divergence in diagram (b) is canceled by (d) [7]. Summing over all polarizations and spins

$$\begin{aligned}|\mathcal{M}^{(^5P_2)}|^2&=5\left(\frac{Z_C M_N}{M}\right)^2\frac{64\pi\,\alpha M^2|h^{(2)}\sqrt{z^{(2)}}|^2}{\mu}\\&\times\left[|1+X|^2-\frac{p^2\sin^2\theta}{p^2+\gamma^2}\left(\frac{2\gamma^2}{p^2+\gamma^2}+X+X^*\right)\right],\\X&=\frac{i}{-1/a_0^{(2)}-ip}(p-i\frac{2}{3}\frac{\gamma^3-ip^3}{p^2+\gamma^2}),\end{aligned} \quad (8)$$

with $\alpha=e^2/(4\pi)$, the dimer polarization sum $\sum\varepsilon_{ij}\varepsilon^*_{xy}=R_{ijxy}$ [19] and the wave function renormalization $h^{(2)2}|z^{(2)}|=2\pi/|3\gamma+r_1^{(2)}|$, where $r_1^{(2)}$ is the effective range in the $^5P_2$ scattering amplitude. $z^{(2)}$ is defined as the residue at the pole in the dressed dimer propagator $D^{(2)}(p_0,\boldsymbol{p})$. The capture from $^3S_1$ to $^3P_2$ state has the same exact expression as Eq. (8) except that $a_0^{(2)}$, $r_1^{(2)}$, and $z^{(2)}$ are replaced by the corresponding parameters in the spin channel 1. The differential cross section averaged over initial spin states is

$$\frac{d\sigma}{d\cos\theta}=\frac{1}{32\pi M^2}\frac{p^2+\gamma^2}{2\mu p}\frac{1}{8}\frac{|\mathcal{M}^{(^5P_2)}|^2+|\mathcal{M}^{(^3P_2)}|^2}{2}, \quad (9)$$

taking the ^{8}Li nucleus as a symmetric combination $(|^3P_2\rangle+|^5P_2\rangle)/\sqrt{2}$ of final states. The total cross section $\sigma(p)$ is calculated with a straightforward integration over the angle θ.

The parameters in $\sigma(p)$ can be determined from elastic n-^{7}Li scattering data and ^{8}Li binding energy. However, the p-wave effective range $r_1^{(\kappa)}$ is not known accurately. This is the main theoretical uncertainty at this order. Changing the effective range $r_1^{(\kappa)}$ modifies $z^{(\kappa)}$ and moves the cross section up or down by a multiplicative factor. In traditional potential model calculations, the parameters are determined by reproducing the ^{8}Li binding energy. However, this does not constrain the effective range and other parameters of the ERE. For example, in a Woods-Saxon potential $V(r)=-v_0[1+\exp(\frac{r-R_c}{a_c})]^{-1}$ different choices for the depth v_0, range R_c, diffusiveness a_c can be made to reproduce the known ^{8}Li binding energy. This however produces different effective ranges, and constitutes an irreducible source of error in the theoretical calculations.

Comparing the contributions to the capture cross section from the two spin channels analytically, we get

$$\frac{\sigma^{(^5P_2)}}{\sigma^{(^5P_2)}+\sigma^{(^3P_2)}}\Big|_{p=0}=\frac{(3-2a_0^{(2)}\gamma)^2}{(3-2a_0^{(2)}\gamma)^2+(3-2a_0^{(1)}\gamma)^2}\approx 0.81, \quad (10)$$

using the same effective range r_1 in both spin channels. This ratio is close to the experimentally observed ratio [20]. From Eqs. (8), (9) one can see that the total cross section at low energy is not independently sensitive to $r_1^{(2)}$ and $r_1^{(1)}$. This is confirmed by our fit to data.

In Fig. 3, we compare potential model calculations using Tombrello's [12], and Davids-Typel's [8] parameters to EFT curves. At low energy the potential model results can be reproduced in EFT with a small variation in the effective range $-0.46\ \text{fm}^{-1}\le r_1\le -0.3\ \text{fm}^{-1}$. At higher energies they differ since potential models include ERE parameters beyond the scattering length and effective range. A fit to data from Ref. [21] in the energy range $E_n\sim 2-700$ eV gives an effective range $r_1=-1.83\ \text{fm}^{-1}$ with only the spin channel 2 contribution and $r_1=-1.47\ \text{fm}^{-1}$ with both spin channels 1 and 2. Both the r_1 values are compatible with the Wigner bound [22] which, for a nucleon-core interaction shorter than 3 fm restricts r_1 to be smaller than around $-1\ \text{fm}^{-1}$. Following Ref. [21], their data and the theory curves in the right panel in Fig. 3 were divided by the known experimental branching ratio 0.89 to the ground state and compared to a few other available data [23–25]. The r_1 was fitted to the unscaled data for transition to the ground state as appropriate. It is clear that the theory error in the low energy extrapolation comes from the uncertainty in the effective range at leading order.

Conclusions: Using a model-independent formalism we demonstrated and quantified the theoretical uncertainty in the ^{7}Li$(n,\gamma)^8$Li calculation associated with phenomenological potentials in the single particle approximation. The leading order result depends on the p-wave effective range parameter r_1 that is poorly known. Without detailed knowledge about this parameter, model calculations deviate from data at low energy. We extract this effective range parameter by fitting our analytic form to data.

It is important to stress that this sensitivity to r_1 at low energies is a consequence of having two operators for shallow p-wave states at leading order. Therefore the conclusions of the present work also apply to the ^{7}Be$(p,\gamma)^8$B reaction. Coulomb

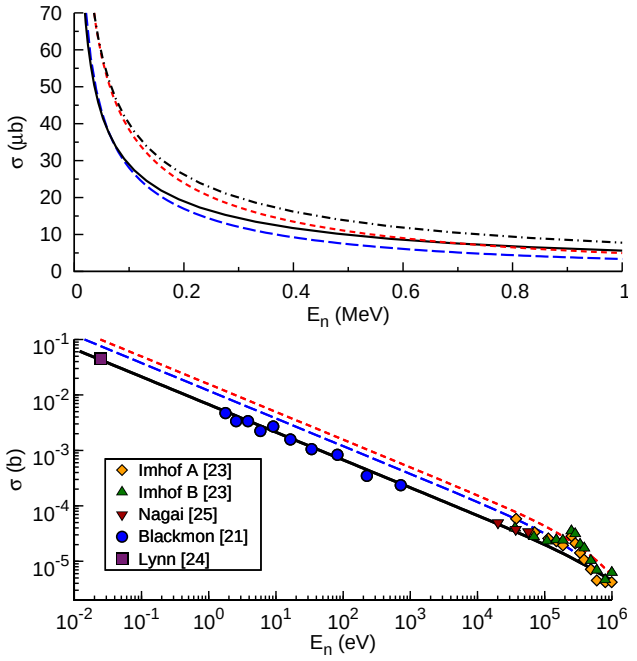

FIG. 3. Potential model curves: (blue) long-dashed curve from Davids-Typel [8], (red) dashed curve from Tombrello [12]. Top panel: (black) solid curve EFT with $r_1 = -0.3$ fm^{-1}, (black) dot-dashed curve EFT with $r_1 = -0.46$ fm^{-1}. Bottom panel: (black) solid curve EFT with r_1 fitted to data.

interactions in $p+{}^7$Be scattering and ${}^7\mathrm{Be}(p,\gamma)^8\mathrm{B}$ reaction is under investigation [26].

The EFT expression for ${}^7\mathrm{Li}(n,\gamma)^8\mathrm{Li}$ capture is consistent with low energy data, which is lower than model calculations [8, 12] as shown. Since this reaction effects ^{7}Li abundances, the impact of the uncertainty in r_1 in inhomogeneous BBN can be explored using our analytic expression.

At higher order in the EFT expansion, the cross section would get corrections from two sources: higher order initial and final state interactions, and two-body currents. The former can be related to the ERE. At the very low energy, it is the final state interactions, which modify the wave function renormalization constants, that are important. At next-to-next-to-leading order the shape parameter associated with p-wave interaction contribute [6, 26]. In addition, at higher order two-body currents such as $E_i(NF_jC)^\dagger[NF_x(\overrightarrow{\nabla}/M_C - \overleftarrow{\nabla}/M_N)_yC]R_{ijxy}$, where E_i is the electric field, contribute. These operators are not constrained by elastic scattering. A higher order EFT calculation would reduce theoretical errors though at the expense of additional parameters. This is not necessarily a drawback as what we gain is a model-independent understanding of the sources of higher order contributions, and a more detailed knowledge about the kind of experimental input that is required to better constrain the low energy theory.

Acknowledgments: The authors thank P. Bedaque, C. Bertulani, B. Davids, V. Guimarães, C. Johnson, A. Mukhamedzhanov, S. Typel for valuable discussions; ECT*, INT, MSU (R.H.) for hospitality; and the HPCC center at MSU (G.R.), the U.S. NSF grant PHY-0969378 (G.R.), the FOM programme 114 (R.H.), the BMBF contract 06BN411 (R.H.) for partial support. Authors are extremely grateful to S. Typel for providing the potential model numbers.

* grupak@u.washington.edu
† R.Higa@rug.nl

[1] S. Burles, K. M. Nollett, J. N. Truran, and M. S. Turner, Phys. Rev. Lett., **82**, 4176 (1999).
[2] C. Rolfs and W. Rodney, *Cauldrons in the Cosmos* (University Of Chicago Press, London, 1988).
[3] S. W. Barwick *et al.*, arXiv:astro-ph/0412544.
[4] E. G. Adelberger *et al.*, Rev. Mod. Phys., **70**, 1265 (1998).
[5] G. Rupak, Nucl. Phys., **A678**, 405 (2000).
[6] C. A. Bertulani, H. W. Hammer, and U. Van Kolck, Nucl. Phys., **A712**, 37 (2002); P. F. Bedaque, H. W. Hammer, and U. van Kolck, Phys. Lett., **B569**, 159 (2003).
[7] D. R. Phillips and H. W. Hammer, EPJ Web Conf., **3**, 06002 (2010).
[8] B. Davids and S. Typel, Phys. Rev. C, **68**, 045802 (2003).
[9] P. Descouvemont, Phys. Rev. C, **70**, 065802 (2004).
[10] The Facility for Rare Isotope Beams (FRIB) at the Michigan State University, http://frib.msu.edu/.
[11] L. H. Kawano, W. A. Fowler, R. W. Kavanagh, and R. A. Malaney, Astrophys. J., **372**, 1 (1991).
[12] T. Tombrello, Nucl. Phys., **71**, 459 (1965).
[13] J. T. Huang, C. A. Bertulani, and V. Guimaraes, At. Data Nuc. Data Tables, **96**, 824 (2010).
[14] L. Trache *et al.*, Phys. Rev. C, **67**, 062801 (2003).
[15] D. B. Kaplan, M. J. Savage, and M. B. Wise, Phys. Lett., **B424**, 390 (1998).
[16] L. Koester, K. Knopf, and W. Waschkowski, Z. Phys., **A312**, 81 (1983); C. Angulo *et al.*, Nucl. Phys., **A716**, 211 (2003).
[17] P. F. Bedaque and U. van Kolck, Phys. Lett., **B428**, 221 (1998); J.-W. Chen, G. Rupak, and M. J. Savage, Nucl. Phys., **A653**, 386 (1999).
[18] S. Typel and G. Baur, Nucl. Phys., **A759**, 247 (2005).
[19] S. Choi, J. Lee, J. S. Shim, and H. Song, J. Korean Phys. Soc., **25**, 576 (1992); S. Fleming, T. Mehen, and I. W. Stewart, Nucl. Phys., **A677**, 313 (2000).
[20] F. C. Barker, Nucl. Phys., **A588**, 693 (1995).
[21] J. C. Blackmon *et al.*, Phys. Rev. C, **54**, 383 (1996).
[22] H. W. Hammer and D. Lee, Annals Phys., **325**, 2212 (2010).
[23] W. L. Imhof, R. G. Johnson, F. J. Vaughn, and M. Walt, Phys. Rev., **114**, 1037 (1959), the two data sets correspond to two different normalizations of the same data.
[24] J. E. Lynn, E. T. Jurney, and S. Raman, Phys. Rev. C, **44**, 764 (1991).
[25] Y. Nagai *et al.*, Phys. Rev. C, **71**, 055803 (2005).
[26] R. Higa and G. Rupak, in preparation.